Int. J. Therm. Sci. (2001) 40, 959–968

S1290-0729(01)01282-0/FLA

Transient conductive–radiative numerical analysis of multilayer thin films heated by different laser pulses

Nicola Bianco [a], Oronzio Manca [b], Vincenzo Naso [a,*]

[a] *Dipartimento di Energetica, Termofluidodinamica applicata e Condizionamenti ambientali, Università degli studi di Napoli Federico II, Piazzale Tecchio 80-80125, Napoli, Italy*

[b] *Dipartimento di Ingegneria Aerospaziale, Seconda Università degli studi di Napoli, Real Casa dell'Annunziata, Via Roma, 29-81031 Aversa (CE), Italy*

(Received 28 July 2000, accepted 9 February 2001)

Abstract — A thermal and optical one-dimensional numerical analysis of semi-transparent single and multilayer thin films on a transparent thermically semi-infinite glass substrate, irradiated by a laser source, is presented, in classical conductive Fourier hypothesis. The absorption is evaluated by means of the classical optical matrix method. Both in thermal and optical models the effects of temperature on the properties are taken into account. A pulsed laser source impinges on the glass side of the structure. Four different typical pulse shapes are compared at the same energy amount: a rectangular on–off shape, a symmetric triangular shape, a Gaussian shape, an asymmetric triangular Weibull profile. Numerical calculations are performed, with reference to a Nd-YAG pulsed laser and to the three structures by means of which an amorphous silicon photovoltaic cell is progressively manufactured: a single transparent conductive oxide SnO_2 (TCO) layer, a double layer of amorphous silicon (a-Si) and TCO, an Al/a-Si/TCO multilayer thin film. In each case the single or composite thin films are on a glass substrate. Results are reported in terms of depth and time profiles of radiative coefficients and temperature. © 2001 Éditions scientifiques et médicales Elsevier SAS

multilayer thin films / pulsed lasers / combined heat transfer / conductive–radiative heat transfer / numerical analysis / radiative coefficients profiles

Nomenclature

A	absorptance	
c	specific heat	$J{\cdot}kg^{-1}{\cdot}K^{-1}$
c'	speed of light	$m{\cdot}s^{-1}$
d	control volume thickness	m
E	electric field	$N{\cdot}C^{-1}$
f	time function	
i	imaginary unit	
I	irradiance	$W{\cdot}m^{-2}$
k	thermal conductivity	$W{\cdot}m^{-1}{\cdot}K^{-1}$
k_{est}	extinction coefficient	
$\mathbf{M}$	transmission matrix	
N	number of layers	
n	real part of refractive index	
$\overline{n}$	complex refractive index	
$\overline{r}$	Fresnel's coefficient	
R	reflectance	
S	Poynting vector	$W{\cdot}m^{-2}$
s	material thickness	m
t	time	s
$\overline{t}$	Fresnel's coefficient	
T	temperature	K
$\dot{u}'''$	absorption function	$W{\cdot}m^{-3}$
z	spatial coordinate	m

Greek symbols

λ	wavelength	m
μ	magnetic permeability	$N{\cdot}s^2{\cdot}C^{-2}$
ρ	density	$kg{\cdot}m^{-3}$
τ	transmittance	

Subscripts

a	air
i	material
in	initial
k	generic control volume
l	pulse length
m	layer

* Correspondence and reprints.
E-mail addresses: nibianco@unina.it (N. Bianco), manca@unina.it (O. Manca), vinaso@unina.it (V. Naso).

p peak
s substrate

Superscripts

t transmitted part
r reflected part
* complex conjugate

1. INTRODUCTION

The growing technological importance of thin films has spurred the deepening of conventional and new manufacturing and treatment processes. In particular, when either pulsed or continuous laser sources are used for annealing, damage of optical coatings, optical recording and scribing of photovoltaic cells, a thorough knowledge of the interaction between the source and the material is necessary for the best design of the process.

Thermal treatment of thin film manufacturing processes with pulsed lasers is a common procedure [1]. In these processes the heat source impinges on a very small area and a high heat flux is obtained, which induces a localised overheating. Since optical properties of thin film materials generally depend on the wavelength of the laser source and on the temperature, a thermally optical nonlinearity occurs. Therefore, the analysis of thermal conductive and optical distributions is important, in order to broaden the field of application and to improve the control of the process.

Optical and thermal fields induced by a pulsed laser source in multilayer thin films on a transparent substrate were studied by several authors. Results of this analysis can be usefully employed in manufacturing of amorphous-silicon photovoltaic cells. A three-dimensional thermal numerical model, for a multilayer thin film structure irradiated by a circular Gaussian laser beam, was proposed by Nakano et al. [2]. They developed a fabrication technique by which the layers of the a-Si solar cells were selectively scribed by a high-power laser beam. A similar analysis was carried out by Kiyama et al. [3], who adopted a non-linear thermal model. A new method, called laser welding and scribing (LWS), was proposed by Kishi et al. [4], who employed a laser pattern technique to manufacture high-yeld integrated-type a-Si solar cells, that did not require a precise control of the laser power. A one-dimensional numerical study for the thermal design of photovoltaic cells manufacturing was presented by Avagliano et al. [5]. Experimental results and predictions from a numerical model were compared in terms of the cut energy flux values. In the numerical study reference was made to the cut energy flux which determines the melting of the material. Predictions by the one-dimensional model differ from those by multi-dimensional models, as it was reported by Bianco and Manca [6]. However, the one-dimensional model was shown to predict quite well the thermal field in the central area of the laser spot and, it can, therefore, be of interest in the applications.

Grigoropoulos et al. [7], in their measurements of the thin polysilicon film reflectivity during continuous wave laser annealing, showed that interference effects significantly enhance the variation of the thin film reflectivity with temperature. Park et al. [8, 9] modelled numerically a probe laser response during a pulse laser heating of a-Si thin films. However, the films were opaque to the pump pulse, so that the interference effects on the temperature distributions could be neglected. The effect of the laser pulse shape was also discussed. Grigoropoulos et al. [10] solved the combined optical-thermal problem: the energy absorption was evaluated by the thin film optical model. The authors took into account the effects of a complex index of refraction continuously varying with the temperature. For a single silicon layer on a substrate, they found that the absorption distribution in the thin film exhibited a periodic variation with depth. Chen and Tien [11] analysed the temperature distribution and the optical response of weakly absorbing thin films with thermally induced optical nonlinearity, subjected to short-pulse laser heating. A transient one-dimensional model was set up to examine the effects of the temperature-dependent optical properties and the non-uniform absorption in a thin film. Xu et al. [12] developed and verified the optical reflection technique for the in-situ monitoring of the transient temperature field during the pulsed excimer laser heating of thin polysilicon films. Data on the thin film complex refractive index at high temperatures was employed in the calculation of the sample transient reflectivity response and in the experimental signal analysis. A numerical conductive heat transfer model for the transient temperature field in the thin film structure was applied. Angelucci et al. [13] studied the conjugate optical-thermal nonlinear problem in multilayer thin films. They took into account the dependence of thermophysical and optical properties on temperature. Bianco et al. [14, 15] compared the back treatment and the front treatment processes in terms of the optical characteristics and temperature distributions of a single TCO (transparent conductive oxide, SnO_2) layer, a-Si/TCO and Al/a-Si/TCO multilayer thin films. Results were obtained by means of an optical and thermal one-dimensional model and were related to a Nd-YAG laser source with a wavelength of 1064 nm. The analysis clearly showed that the back treatment is more efficient in manufacturing of photovoltaic cells.

In this paper a simple one-dimensional model is employed to compare the values of process parameters determined by different time shapes of the laser pulse. The objective is to set up a useful tool for those interested in choosing the best shape of the laser pulse for applications. The thermal and optical analysis of semi-transparent single and multilayer thin films on a transparent thermically semi-infinite glass substrate, irradiated by a laser source, is presented, in classical conductive Fourier hypothesis. The absorption is evaluated by means of the optical matrix method. Both in thermal and optical models the effects of temperature on the properties are taken into account. With reference to the manufacturing process of photovoltaic cells, a Nd-YAG pulsed laser source with a 1064 nm wavelength is considered in this paper. A comparison is carried out, at the same energy amount, among four commonly used pulse shapes: a rectangular on-off shape, a symmetric triangular shape, a Gaussian shape, an asymmetric triangular Weibull profile. The laser source impinges uniformly on the glass side of the multilayer structure. Numerical calculations are performed for a single transparent conductive oxide SnO_2 (TCO) layer, a double layer of amorphous silicon (a-Si) and TCO and an Al/a-Si/TCO multilayer thin film. In each case the single or composite thin films are on a glass substrate. Results are reported in terms of depth and time profiles of radiative coefficients and temperature.

2. THERMAL AND OPTICAL ANALYSIS

The basic sketch of the investigated structure is shown in *figure 1(a)*. It consists of a thin multilayer film deposited on a glass substrate. The thickness of the film is far smaller than that of the glass and the substrate can be assumed to be thermally semi-infinite. The solid structure is irradiated by a Q-switched Nd-YAG laser beam. The order of magnitude of the thermal diffusivity of the materials which constitute the multilayer thin film is 10^{-5} m^2·s^{-1} for the TCO and the Al and 10^{-7} m^2·s^{-1} for the glass and the a-Si. The overall thickness of the multilayer film is 1.3 μm, which is practically negligible compared to the laser beam diameter (100 μm), and, therefore, one can assume that the thermal field at the center of the beam is one-dimensional, as it was suggested by Grigoropoulos [1] and shown by Bianco and Manca [6]. At the ns time scales considered in this work, non-equilibrium and non-Fourier thermal wave effects are negligible [1, 11].

With reference to *figure 1(a)*, the one-dimensional heat conduction equation is

$$\frac{\partial}{\partial z_i}\left(k_i(T_i)\,\frac{\partial T_i}{\partial z_i}\right) + \dot{u}'''(T_i, z_i, t) = \rho_i c_i(T_i)\,\frac{\partial T_i}{\partial t} \quad \begin{cases} i = 1, 2, \ldots, N+1 \\ \text{for } 0 \leqslant z_i \leqslant s_i \end{cases} \tag{1}$$

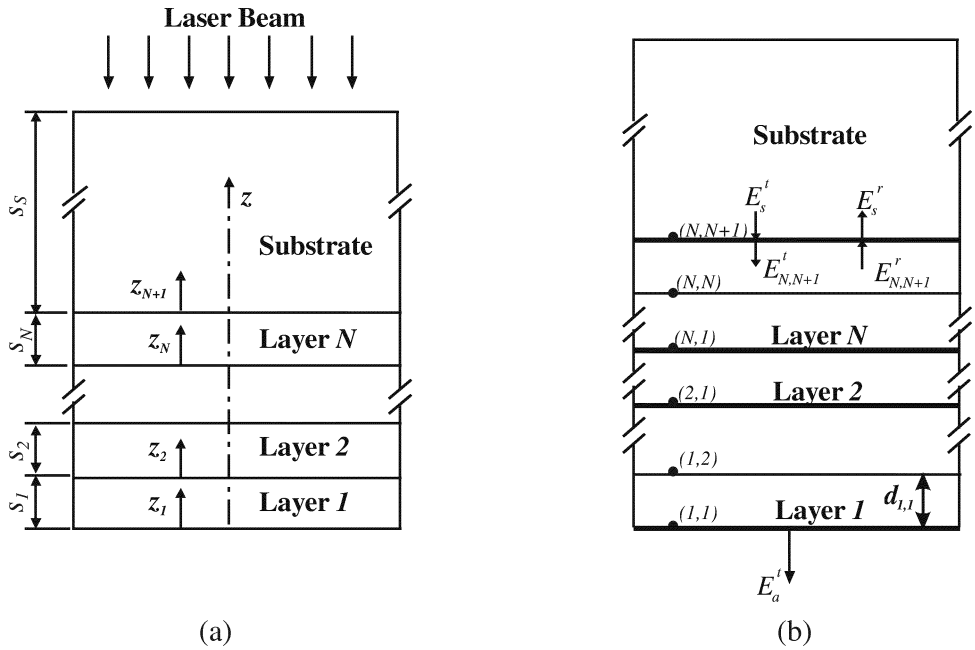

Figure 1. Sketch of the multilayer structure (a), and of the discretization for the optical model (b).

In this work, the dependence of thermophysical properties on the temperature is taken into account. The energy losses due to radiation and convection to the ambient are negligible with respect to the energy absorbed in the considered films [11]. This way, the thin film surface can be assumed to be adiabatic.

The initial and the boundary conditions are

$$T_i(z_i, 0) = T_{\text{in}} \quad \text{for } i = 1, 2, \ldots, N+1 \text{ and } 0 \leqslant z_i \leqslant s_i \tag{2a}$$

$$\frac{\partial T_1(0,t)}{\partial z_1} = 0 \quad \text{for } t \geqslant 0 \tag{2b}$$

$$k_{i-1}(T_{i-1}) \frac{\partial T_{i-1}(s_{i-1}, t)}{\partial z_{i-1}} = k_i(T_i) \frac{\partial T_i(0,t)}{\partial z_i} \quad \text{for } i = 1, 2, \ldots, N+1 \text{ and } t \geqslant 0 \tag{2c}$$

$$T_{i-1}(s_{i-1}, t) = T_i(0, t) \quad \text{for } i = 1, 2, \ldots, N+1 \text{ and } t \geqslant 0 \tag{2d}$$

$$T_{N+1}(z_{N+1} \to \infty, t) = T_{\text{in}} \quad \text{for } t \geqslant 0 \tag{2e}$$

The energy absorption term $\dot{u}'''(T_i, z_i, t)$ is related to the Poynting vector and depends on the optical properties of the materials. It can be evaluated, together with the reflectance and the transmittance of the structure, according to Chen and Tien [11]. All interfaces are assumed to be optically smooth. The temperature dependence on optical properties determines a non uniform distribution of the refractive index in the film; each layer of the thin film structure is treated as a multilayer composed of N_m layers of varying complex refractive index $\overline{n}$. A plane, monochromatic and linearly polarized wave with amplitude of the electric field E_{s}^{t} is ortogonally incident on the structure, *figure 1(b)*. The corresponding energy flow along the x-direction is

$$S = \frac{n_{\text{s}}}{2\mu c'} E_{\text{s}}^{\text{t}^2} \tag{3}$$

where n_{s} is the real part of the glass refractive index.

The complex refractive index of the kth layer of thickness $d_{m,k}$, in the mth material is $\overline{n}_{m,k} = n_{m,k} - \text{i}k_{\text{est}\,m,k}$. The relation between the transmitted and reflected electric fields, $E_{m,k}^{\text{t}}$ and $E_{m,k}^{\text{r}}$, at the kth interface is

$$\begin{pmatrix} E_{m,k-1}^{\text{t}} \\ E_{m,k-1}^{\text{r}} \end{pmatrix} = \mathbf{M}_{m,k} \begin{pmatrix} E_{m,k}^{\text{t}} \\ E_{m,k}^{\text{r}} \end{pmatrix} \tag{4}$$

where $\mathbf{M}_{m,k}$ is the transmission matrix of the kth control volume in the mth material defined as:

$$\mathbf{M}_{m,k} = \frac{1}{\overline{t}_{m,k-1}} \times \begin{bmatrix} \exp\left(\text{i}\frac{2\pi}{\lambda}\overline{n}_{m,k}d_{m,k}\right) & \overline{r}_{m,k-1}\exp\left(-\text{i}\frac{2\pi}{\lambda}\overline{n}_{m,k}d_{m,k}\right) \\ \overline{r}_{m,k-1}\exp\left(\text{i}\frac{2\pi}{\lambda}\overline{n}_{m,k}d_{m,k}\right) & \exp\left(-\text{i}\frac{2\pi}{\lambda}\overline{n}_{m,k}d_{m,k}\right) \end{bmatrix} \tag{5}$$

In the previous expression $\overline{r}_{m,k-1}$ and $\overline{t}_{m,k-1}$ are the Fresnel's coefficients defined as:

$$\overline{t}_{m,k-1} = \frac{2\overline{n}_{m,k-1}}{\overline{n}_{m,k-1} + \overline{n}_{m,k}} \tag{6a}$$

$$\overline{r}_{m,k-1} = \frac{\overline{n}_{m,k-1} - \overline{n}_{m,k}}{\overline{n}_{m,k-1} + \overline{n}_{m,k}} \tag{6b}$$

The multilayer transmission matrix $\mathbf{M}$ is

$$\mathbf{M} = \prod_{m=1}^{N} \prod_{k=1}^{N_m} \mathbf{M}_{m,k} \tag{7}$$

It is possible to evaluate E_{a}^{t} and E_{s}^{r} by means of the relation

$$\begin{pmatrix} E_{\text{s}}^{\text{t}} \\ E_{\text{s}}^{\text{r}} \end{pmatrix} = \mathbf{M} \begin{pmatrix} E_{\text{a}}^{\text{t}} \\ 0 \end{pmatrix} \tag{8}$$

The determination of $E_{m,k}^{\text{t}}$ and $E_{m,k}^{\text{r}}$ can be obtained by inverting equation (4).

The power density in the kth control volume is given by the Poynting vector

$$S_{m,k} = \frac{1}{2\mu c'} \text{Re}\left[\left(\overline{n}_{m,k}\right)^* \left(E_{m,k}^{\text{t}} + E_{m,k}^{\text{r}}\right) \times \left(E_{m,k}^{\text{t}} - E_{m,k}^{\text{r}}\right)^*\right] \tag{9}$$

and the absorbed power per unit volume is

$$\dot{u}_{m,k}''' = f(t) \frac{\text{d}S_{m,k}}{\text{d}z} \tag{10}$$

where $f(t)$ is a function of the time, which characterises the time shape of the pulse.

The radiative coefficients of the overall multilayer film, R, τ, and A, can be evaluated by the following equations:

$$R = \frac{|E_{\text{s}}^{\text{r}}|^2}{|E_{\text{s}}^{\text{t}}|^2} \tag{11}$$

$$\tau = \frac{n_{\text{a}}|E_{\text{a}}^{\text{t}}|^2}{n_{\text{s}}|E_{\text{s}}^{\text{t}}|^2} \tag{12}$$

$$A = 1 - R - \tau \tag{13}$$

The numerical procedure was tested in [13].

TABLE I
Optical and thermophysical properties of the materials.

Material	Properties			
	k [W·m·K^{-1}]	c [J·kg^{-1}·K^{-1}]	ρ [kg·m^{-3}]	$\overline{n} = n - ik_{est}$
Glass	1.4 [10]	1200 [10]	2200 [10]	1.0 − i0.0 [Assumed]
TCO	$39.6 - 2.09 \times 10^{-2}(T - 273.15) + 4.62 \times 10^{-6}(T - 273.15)^2$ [3]	$371.0 + 0.217(T - 273.15)$ [3]	6640 [3]	1.95 − i0.002 [3]
a-Si	$1.3 \times 10^{-9}(T - 900)^3 + 1.3 \times 10^{-7}(T - 900)^2 + 10^{-4}(T - 900) + 1.0$ [16]	$952.0 + (171.0 \cdot T)/685$ [3]	2330 [3]	$3.8 - i[0.0443 + 6.297 \times 10^{-5} \times (T - 273.15)]$ [17]
Al	$275 - 0.213(T - 273.15) + 1.55 \times 10^{-4}(T - 273.15)^2$ [3]	$753 + 0.49 \times 10^{-3} T$ [3]	2660 [3]	2.0 − i12.0 [3]

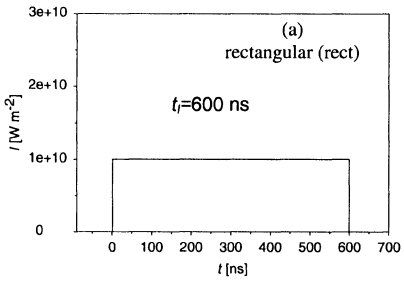

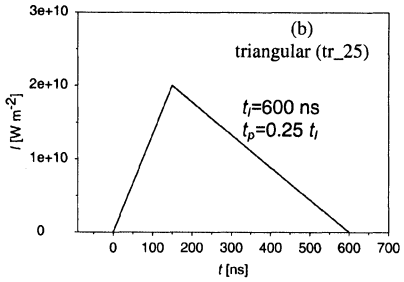

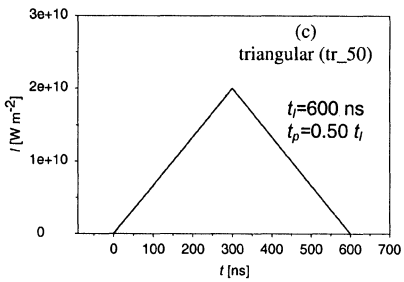

$$f(t) = \begin{cases} 1 & \text{for } 0 \le t \le t_l \\ 0 & \text{for } t > t_l \end{cases}$$

$$f(t) = \begin{cases} t/t_p & \text{for } 0 \le t \le t_p \\ \dfrac{(t_l - t)}{(t - t_p)} & \text{for } t_p \le t \le t_l \\ 0 & \text{for } t > t_l \end{cases}$$

$$f(t) = \begin{cases} t/t_p & \text{for } 0 \le t \le t_p \\ \dfrac{(t_l - t)}{(t - t_p)} & \text{for } t_p \le t \le t_l \\ 0 & \text{for } t > t_l \end{cases}$$

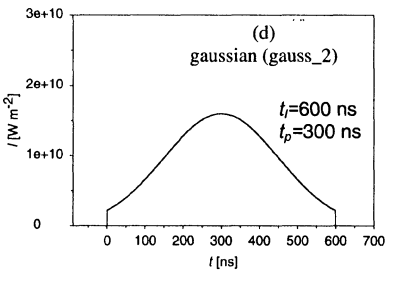

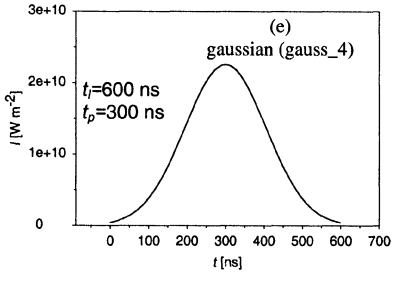

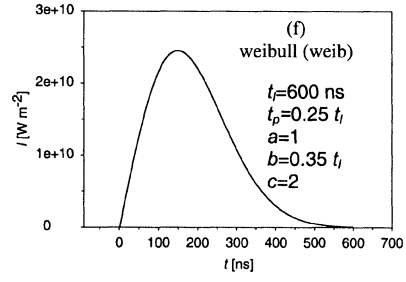

$$f(t) = \exp\left[-2 \times \frac{(t - t_p)^2}{t_p^2}\right]$$

$$f(t) = \exp\left[-4 \times \frac{(t - t_p)^2}{t_p^2}\right]$$

$$f(t) = a\left(\frac{c-1}{c}\right)^{\frac{1-c}{c}}\left[\frac{t - t_p}{b} + \left(\frac{c-1}{c}\right)^{\frac{1}{c}}\right]^{c-1} \exp\left\{-\left[\frac{t - t_p}{b} + \left(\frac{c-1}{c}\right)^{\frac{1}{c}}\right]^{c}\right\}$$

Figure 2. Irradiance vs time, for different shapes of the pulse laser: (a) rectangular; (b) triangular 25; (c) triangular 50; (d) Gaussian 2; (e) Gaussian 4; (f) Weibull.

3. RESULTS

In this paper calculations are carried out for a single layer of a Transparent Conductive Oxide (TCO) SnO_2, an a-Si/TCO double layer and an Al/a-Si/TCO multilayer thin film. The thickness of the Al, the TCO and the a-Si layer are 0.20 μm, 0.60 μm and 0.50 μm, respectively. In each case the film is deposited on a glass substrate. The optical and thermal properties of the materials are reported in *table I*. The laser irradiation wavelength is 1.064 μm. The duration of the ON period is 600 ns. For all the chosen laser shapes (a rectangular on–off shape, a symmetric triangular shape, a Gaussian shape and an asymmetric triangular Weibull profile) an amount of the energy flux irradiated on the material (fluence) equal to 6.0 $kJ \cdot m^{-2}$ is assumed, which is typically employed in photovoltaic cells manufacturing process [5]. The irradiance profiles as a function of time are presented in *figure 2*.

The calculated values of the radiative coefficients as a function of time, for the a-Si/TCO/glass structure and different pulse shapes, are presented in *figure 3*. All the coefficients are time dependent, because of the dependence of thermophysical properties on the temperature. Apart from the case of the rectangular laser pulse, where the irradiance is uniform, in all other cases, where the laser irradiation increases with the time, the radiative coefficients exhibit increasing slopes, which are determined by the gradual increase in the temperature. *Figure 3(a)* points out that the maximum increase in the absorptance is about 70% of its initial value. The rectangular laser shape induces a nearly linear pattern of the absorptance; the slight decrease in the slope is determined by the uniformity of the irradiance. With different laser shapes the maximum value of A is always attained within the ON time period, at a time which depends on the pulse shape. The difference between the maximum values of the absorptance is nearly 5%. *Figure 3 (b)* and *(c)* show similar profiles of the reflectance and of the transmissivity, which attain their minimum values at the time when the maximum absorptance is attained.

The calculated values of the radiative coefficients as a function of the time, for the Al/a-Si/TCO/glass structure and different laser shapes, are presented in *figure 4*. The absorptance profiles are similar to those of the previous case, apart from the slope at the end of the ON period of the heat source, which is less than for the previous structure. The absorptance values are larger than those for a-Si/TCO, since the aluminium makes the structure opaque, thus enhancing the amount of absorbed energy and, consequently, raising the temperature and, on turn, the absorptance. For the same reason, the reflectance values are lower than in the previous case.

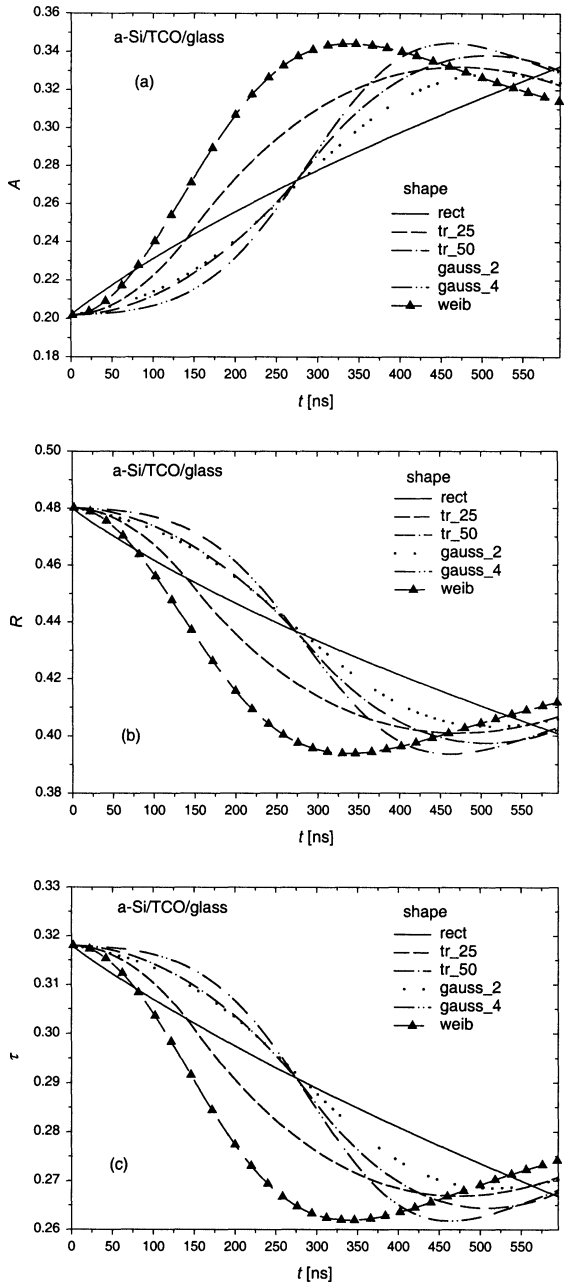

Figure 3. Radiative coefficients vs time, for the a-Si/TCO/glass structure: (a) absorptance; (b) reflectance; (c) transmittance.

The temperature profiles at the TCO surface as a function of time, for the TCO/glass structure and for different laser shapes, are presented in *figure 5*. The surface tem-

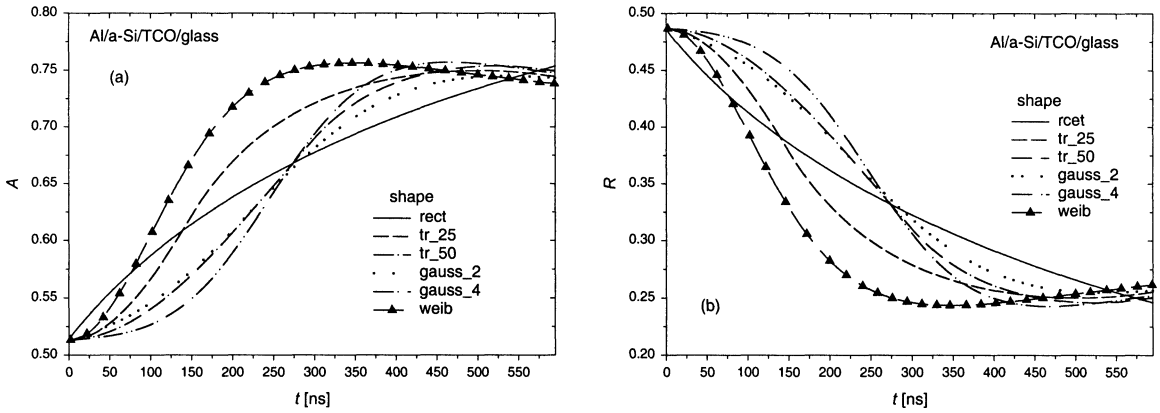

Figure 4. Radiative coefficients vs time, for the Al/a-Si/TCO/glass structure: (a) absorptance; (b) reflectance.

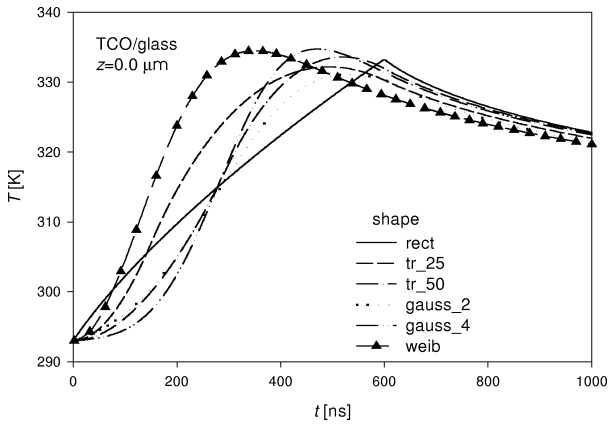

Figure 5. Temperature profiles vs time at the TCO surface, for the TCO/glass structure.

perature of the TCO layer, which is practically isothermal due to its high thermal conductivity, exhibits its maximum value at a time that depends on the laser shape. The maximum is attained at the end of the ON period when the pulse shape is rectangular whereas in the other cases it occurs within the ON period, somewhat later than the time when the laser source has released the maximum irradiation. The maximum temperature values are nearly independent of the laser shape. As far as the slope of the temperature profiles is concerned, we can remark that the rectangular pulse shape releases at the beginning of the process a larger amount of energy than other pulse shapes, apart from the Weibull shape, thus yielding the steepest slope. The time response of the temperature profile is the shortest for the Weibull laser shape, which releases a large fraction of the total energy amount at the beginning of the pulse period.

The temperature profiles as a function of the depth, for the TCO/glass structure and for different laser shapes, are presented in *figure 6*. The figure shows that TCO is practically isothermal at any time; the fair temperature gradient is determined by the heat diffusion to the glass. The sharp variation in the slope of temperature profiles at the TCO/glass interface is due to the very different thermal conductivity values of the materials. The temperature level in the TCO is strongly affected by the laser shape and it is worth noticing that, obviously, the higher the temperature in the TCO the greater the discontinuity in the slope at the TCO/glass interface. In these cases, care has to be taken in manufacturing processes, in order to avoid thermal stress damaging the glass. *Figure 6(b)* points out that at the end of the ON period, when the same amount of energy has been released to the structure by each laser source, differences in temperature profiles are small.

The temperature profiles as a function of the time, for the a-Si/TCO/glass structure and for different laser shapes, are presented in *figure 7*. The temperature profile at the surface of the a-Si layer is similar to the previous ones but the temperature values are larger, because the absorbed energy is greater in this case. The difference between the maximum temperature in the Weibull and the Gaussian 2 profiles, in *figure 7(b)*, is 122 K. As a matter of fact, the Weibull laser shape releases the major part of the energy to the material when its temperature is still relatively low. *Figure 7(b)* shows that at the a-Si/TCO interface ($z = 0.6$ μm) differences in the temperatures for various laser shapes are smaller than at the surface and the maximum temperature is always attained at the end of the ON period.

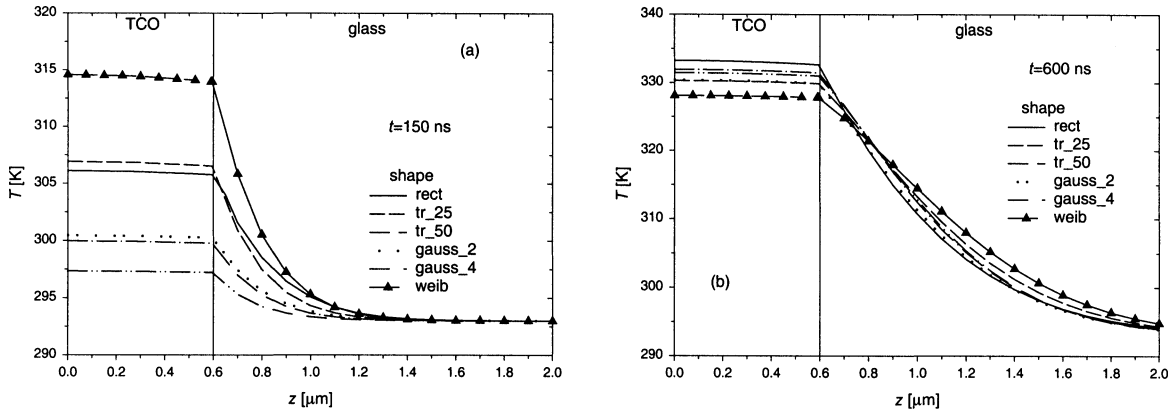

Figure 6. Temperature profiles vs depth, for the TCO/glass structure and for different laser shapes: (a) $t = 150$ ns; (b) $t = 600$ ns.

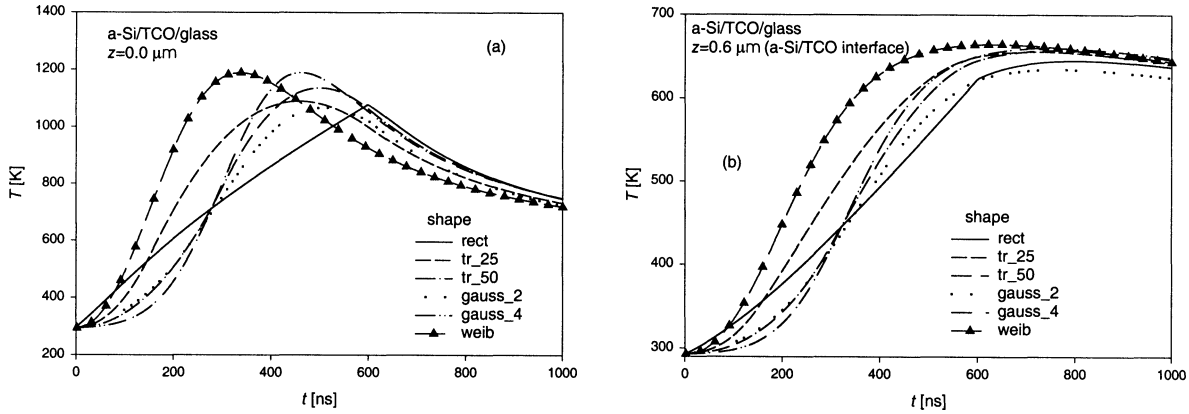

Figure 7. Temperature profiles vs time, for the a-Si/TCO/glass structure and for different laser shapes: (a) $z = 0.0$ μm; (b) $z = 0.6$ μm.

The temperature profiles as a function of the depth, for the a-Si/TCO/glass structure and for different laser shapes, are presented in *figure 8*. In *figure 8(a)* one can notice that interference phenomena in the material induce some oscillations along the depth in the temperature profiles, which are more marked for the Weibull and the triangular 25 shapes, since in these cases the maximum amount of energy is released at $t = 150$ ns. As already pointed out for the TCO/glass structure in *figure 6*, one can observe a sharp discontinuity in the temperature profiles at the a-Si/TCO and TCO/glass interfaces.

The temperature profiles as a function of the time, for the Al/a-Si/TCO/glass structure and for different laser shapes, are presented in *figure 9*. The aluminium layer determines temperature values much larger than those in the previous cases, at both depths, as already noticed with reference to the absorptance. It is worth remarking that in all cases aluminium melting occurs, at different times, which depend on the pulse shape. It is plain that after that time the prediction of this thermal model is not reliable and, therefore, the model must be modified to take the effects of melting into account. *Figure 9(b)* shows that the temperature at the a-Si/TCO interface still increases after the end of the ON period, for the reason that will be realized observing the next figure.

The temperature profiles as a function of the depth, for the Al/a-Si/TCO/glass structure and for different laser shapes, are presented in *figure 10*. *Figure 10(a)* shows that at $t = 150$ ns the maximum temperature is always attained in the inner part of the a-Si, because of the heat diffusion from the a-Si both to the aluminium and to the TCO. Also in this case some interference in the temperature profiles can be noticed. At the end of the ON period differences in the temperature profiles are less marked and temperature gradients in the a-Si are dampened. As already pointed out in comments on

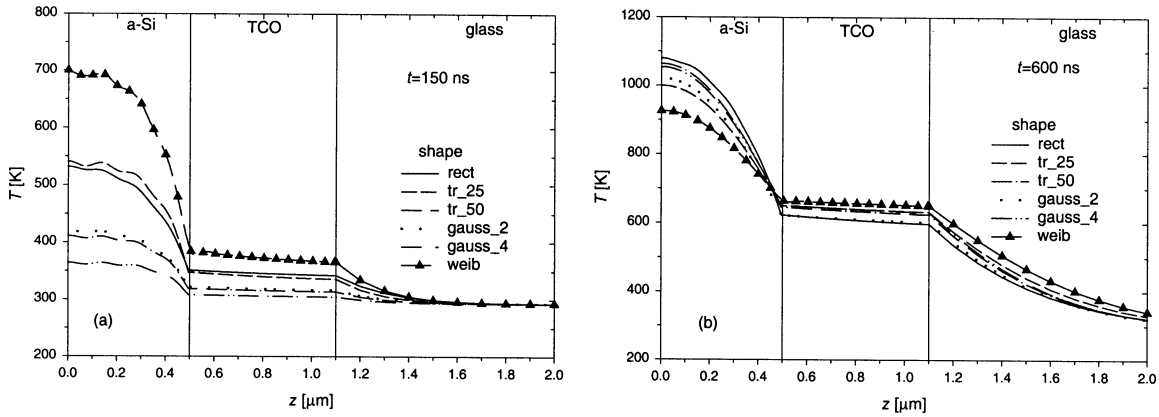

Figure 8. Temperature profiles vs depth, for the a-Si/TCO/glass structure and for different laser shapes: (a) $t = 150$ ns; (b) $t = 600$ ns.

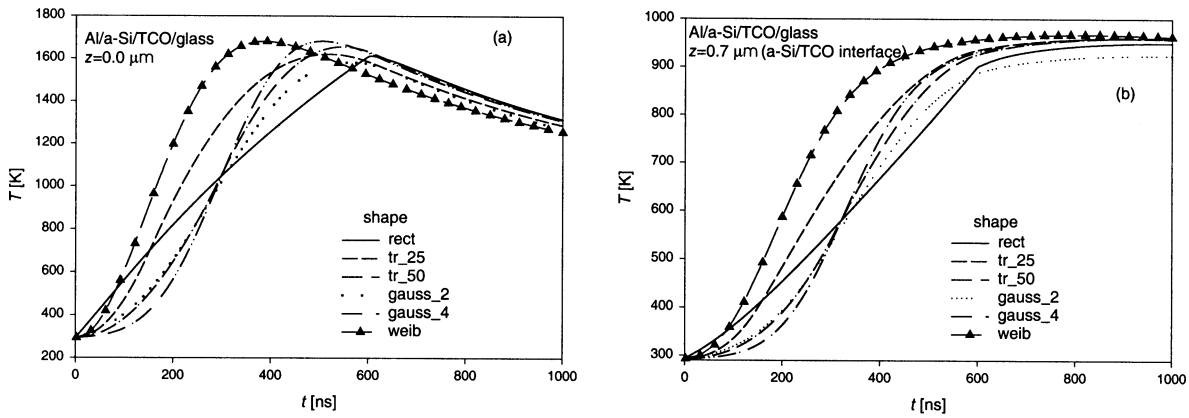

Figure 9. Temperature profiles vs time, for the Al/a-Si/TCO/glass structure and for different laser shapes: (a) $z = 0.0$ μm; (b) $z = 0.7$ μm.

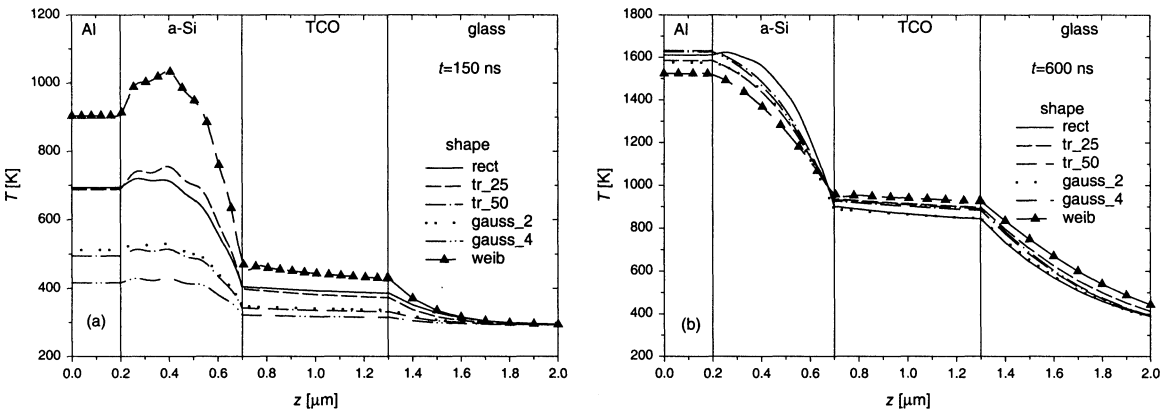

Figure 10. Temperature profiles vs depth, for the Al/a-Si/TCO/glass structure and for different laser shapes: (a) $t = 150$ ns; (b) $t = 600$ ns.

figure 9, during the heat treatment aluminium has melted and also the temperature attained in the a-Si layer is greater than its melting temperature, according to the present model. However, whether it really occurs or not could be correctly predicted only by the afore-mentioned modified model.

4. CONCLUSIONS

The nonlinearity of the conjugate radiative–conductive thermal field causes the radiative coefficients (absorptance, reflectance, transmittance) to be dependent also on the time pattern of the laser source. Absorptance values 1.7 and 1.5 larger than the initial values have been predicted, respectively for the a-Si/TCO/glass and the Al/a-Si/TCO/glass.

In all the examined structures, the higher maximum temperature values are attained for the Weibull shape of the laser source and, moreover, they are achieved earlier than for other laser profiles. On the contrary, the rectangular shape induces the most gradual temperature increase. Therefore, in the laser scribing of a-Si photovoltaic cells a Weibull shape could be preferred, provided the thermal stresses do not damage the material. Among the other laser shapes examined the largest temperatures with smoother slopes in the temperature profiles can be attained using the gauss_4 laser shape.

At the TCO/glass interface in the TCO/glass structure and both at the a-Si/TCO and at TCO/glass interfaces in the Al/a-Si/TCO/glass structure large discontinuities in the slope of temperature profiles are predicted, which could induce dangerous thermal stresses in the TCO and in the glass.

Acknowledgements

This work was supported by a grant from Regione Campania by means of Legge 41/1994. N. Bianco acknowledges Università degli studi di Napoli Federico II and FSE for his fellowship.

REFERENCES

[1] Grigoropoulos C.P., Heat transfer in laser processing of thin films, in: Tien C.L. (Ed.), Annual Review of Heat Transfer, CRC Press, Boca Raton, 1994, pp. 77–130, Chapter 2.

[2] Nakano S., Matsuoka T., Kiyama S., Kawata H., Nakamura N., Nakashima Y., Tsuada S., Nishiwaki H., Ohnishi M., Nagakoa I., Kuwano Y., Laser patterning method for integrated type a-Si solar cell submodules, Japan J. Appl. Phys. 25 (1986) 1936–1943.

[3] Kiyama S., Hirono Y., Hosokawa H., Moriguchi T., Nakano S., Osumi M., Temperature distribution analysis in multilayer thin film structures by laser beam irradiation, Japan Soc. Precision Engrg. 56 (1990) 1500–1506.

[4] Kishi Y., Murata K., Inou H., Kiyama S., Ohnishi M., Nakano S., Kuwano Y., A laser welding and scribing (LWS) method for a high-yield integrated-type, Japan J. Appl. Phys. 30 (1991) 1628–1634.

[5] Avagliano S., Bianco N., Manca O., Naso V., Combined thermal and optical analysis of laser back-scribing for amorphous-silicon photovoltaic cells processing, Internat. J. Heat Mass Trans. 42 (1998) 645–656.

[6] Bianco N., Manca O., Two-dimensional transient analysis of absorbing thin films in laser treatments, ASME J. Heat Trans. 122 (2000) 113–117.

[7] Grigoropoulos C.P., Dutcher W.E., Barclay K.E., Radiative phenomena in CW laser annealing, ASME J. Heat Trans. 113 (1991) 657–662.

[8] Park H.K., Xu X., Grigoropoulos C.P., Do N., Klees L., Leung P.T., Tam A.C., Temporal profile of optical transmission probe for pulsed-laser heating of amorphous films, Appl. Phys. Lett. 61 (1992) 749–751.

[9] Park H.K., Xu X., Grigoropoulos C.P., Do N., Klees L., Leung P.T., Tam A.C., Transient optical transmission measurement in excimer-laser irradiation of amorphous silicon films, ASME J. Heat Trans. 115 (1993) 178–183.

[10] Grigoropoulos C.P., Park H.K., Xu X., Modelling of pulsed laser irradiation of thin film silicon layers, Internat. J. Heat Mass Trans. 36 (1993) 919–924.

[11] Chen G., Tien C.L., Thermally induced optical nonlinearity during transient heating of thin films, ASME J. Heat Trans. 116 (1994) 311–316.

[12] Xu X., Grigoropoulos C.P., Russo R.E., Transient temperature during pulse excimer laser heating of thin polysilicon films obtained by reflectivity measurement, ASME J. Heat Trans. 117 (1995) 17–24.

[13] Angelucci N., Bianco N., Manca O., Thermal transient analysis of thin film multilayers heated by pulsed laser, Internat. J. Heat Mass Trans. 40 (1997) 4487–4491.

[14] Bianco N., Morrone B., Manca O., Conjugate optical-thermal models of back and front laser treatments of thin multilayer films, Heat Technology 15 (1997) 49–56.

[15] Bianco N., Manca O., Morrone B., Instationary conjugate optical-thermal fields in thin films due to laser heating: a comparison between back and front treatment, Heat Mass Trans. 34 (1998) 255–261.

[16] Ong C.K., Tan H.S., Sin E.H., Calculation of melting threshold of crystalline and amorphous materials due to pulsed-laser irradiation, Mat. Sci. Engrg. 79 (1986) 79–85.

[17] Do N., Klees L., Leung P.T., Tong F., Leung W.P., Tam A.C., Temperature dependence of optical constants for amorphous silicon, Appl. Phys. Lett. 60 (1992) 2186–2188.